

Generalized Constant Current Method for Determining MOSFET Threshold Voltage

Matthias Bucher, Nikolaos Makris, and Loukas Chevas

Abstract—A novel method for extracting threshold voltage and substrate effect parameters of MOSFETs with constant current bias at all levels of inversion is presented. This generalized constant-current (GCC) method exploits the charge-based model of MOSFETs to extract threshold voltage and other substrate-effect related parameters. The method is applicable over a wide range of current throughout weak and moderate inversion and to some extent in strong inversion. This method is particularly useful when applied for MOSFETs presenting edge conduction effect (subthreshold hump) in CMOS processes using Shallow Trench Isolation (STI).

constant current method, charge-based model, edge conduction, MOSFET, parameter extraction, threshold voltage

I. INTRODUCTION

Constant current (CC) methods for the extraction of MOSFET threshold voltage are very convenient due to their simplicity, when compared to classical methods using typically extrapolation of drain current in strong inversion. However, CC methods often use a somewhat arbitrary current criterion to determine threshold voltage, e.g., $I_{Th} = 100nA \cdot (W/L)$ [1], [2], [3]. This current criterion is then applied to measured transfer characteristics ($I_D - V_G$) of MOSFETs, from which threshold voltage may be determined as a function of back-bias voltage. CC methods are simple and robust, but the resulting parameters depend on the current criterion used. In [4], [5], the current criterion is established such that the transistor operates in the middle of moderate inversion. The aim of this work is to present a generalization of the current criterion to any level of current, from weak through moderate and to strong inversion. As will be shown, using this generalized current criterion, threshold voltage can be determined from transfer characteristics at any level of current. Hence, the method will be termed generalized constant current (GCC) method. The procedure relies on the charge-based model formulation [6], [7], and enables extracting threshold voltage and other substrate effect related parameters. Note that the adjusted-constant current (ACC) method [5] allows for the determination of threshold voltage from linear to fully saturated operating conditions. Linear mode operation brings benefits in minimizing the impact of second-order effects on the extracted parameters, such as velocity saturation (VS), channel length modulation (CLM), and drain induced barrier lowering (DIBL). The GCC

method presented here concentrates on saturated operating conditions as a generalization of [4]. As will be discussed, the GCC method is preferably applied at weak and moderate levels of inversion, and hence the impact of effects such as VS and CLM are kept minimal.

A particular field of application of the GCC method is the characterization of edge conduction (or "subthreshold hump") effect in MOSFETs. The latter effect often arises in technologies using shallow-trench isolation (STI) schemes. As will be shown, the GCC method is a powerful tool to determine parameters for the edge conduction effect.

II. GENERALIZED CONSTANT CURRENT METHOD IN WEAK AND MODERATE INVERSION

The generalized constant current method to extract threshold voltage is intricately linked with the charge-based model approach [6], [7]. In the latter, drain current is written,

$$I_D = I_{spec} (i_f - i_r) = I_{spec} (q_s^2 + q_s - q_d^2 - q_d) \quad (1)$$

where $i_{f(r)} = q_{s(d)}^2 + q_{s(d)}$ are the normalized forward(reverse) current components depending on the inversion charge densities $q_{s(d)}$ at source(drain), respectively. The same relationship can also be reversed as $q_{s(d)} = \sqrt{1/4 + i_{f(r)}} - 1/2$. The specific current I_{spec} is defined as,

$$I_{spec} = I_0 \cdot (W/L) = 2nU_T^2 \mu C_{ox} (W/L) \quad (2)$$

which may be obtained from measurement as in [4], [5]. In the above, n is the slope factor, mobility is μ , and $C_{ox} = \epsilon_{ox}/T_{ox}$ the gate capacitance depending on oxide thickness T_{ox} . The voltage-charge relationship is expressed as [6],

$$(V_P - V_{S(D)})/U_T = v_p - v_{s(d)} = 2q_{s(d)} + \ln(q_{s(d)}) \quad (3)$$

where voltages $v_p = V_P/U_T$ and $v_{s(d)} = V_{S(D)}/U_T$ may be normalized to the thermal voltage $U_T = kT/q$. The pinch-off voltage V_P is a function of the gate voltage V_G [6]- [8],

$$\begin{aligned} V_P &= V_G - V_{FB} - \Psi_0 - \gamma \left[\sqrt{V_G - V_{FB} + \left(\frac{\gamma}{2}\right)^2} - \frac{\gamma}{2} \right] \\ &\cong (V_G - V_{TO})/n(V_G) \end{aligned} \quad (4)$$

where V_{FB} is the flat-band voltage, $\gamma = \sqrt{2q\epsilon_{si}N_{sub}}/C_{ox}$ is the substrate effect factor, $\Psi_0 \cong 2\Phi_F + 2...3U_T$ is slightly above twice the Fermi potential $\Phi_F = U_T \ln(N_{sub}/n_i)$, N_{sub} and n_i are substrate doping and intrinsic concentrations, and $V_{TO} = V_{FB} + \Psi_0 + \gamma\sqrt{\Psi_0}$ is the threshold voltage.

This work was partly supported under Project INNOVATION-EL-Crete (MIS 5002772).

M. Bucher, N. Makris and L. Chevas are with the School of Electrical and Computer Engineering, Technical University of Crete, 73100 Chania, Greece. (e-mail: bucher@electronics.tuc.gr).

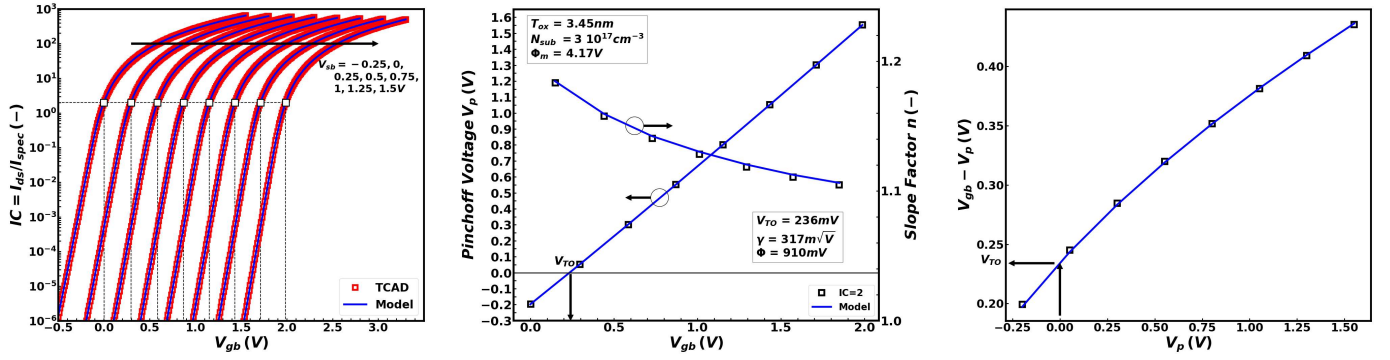


Fig. 1. Principle of the generalized constant current (GCC) method using $IC = 2$ in moderate inversion. Transfer characteristics I_D vs. V_G with applied constant current (left), extracted pinchoff voltage V_P and slope factor n vs. V_G (center) and V_{TO} vs. V_P (right) of a wide/long n-MOSFET in saturation at room temperature. V_{TO} is determined as $V_G|_{V_P=0}$. Both TCAD and model use a constant, non field-dependent mobility. The GCC method is applied in the same way to TCAD data (markers) and charge-based model (lines).

The inverse function $V_G(V_P)$ [8], [9] is equally useful,

$$V_G = V_{TO} + V_P + \gamma \left[\sqrt{\Psi_0 + V_P} - \sqrt{\Psi_0} \right] \quad (5)$$

as it allows us to define both the gate threshold voltage $V_{TB} \equiv V_G|_{V_P=V_S}$ (referred to local substrate), as well as the commonly used threshold voltage V_{TH} (referred to source),

$$V_{TH} \equiv V_G - V_P|_{V_P=V_S} = V_{TO} + \gamma \left[\sqrt{\Psi_0 + V_P} - \sqrt{\Psi_0} \right] \quad (6)$$

The slope factor n is defined as,

$$n \equiv \left[\frac{\partial V_P}{\partial V_G} \right]^{-1} = 1 + \frac{\gamma}{2\sqrt{V_P + \Psi_0}} \quad (7)$$

The combination of (1)-(4) and (7) defines the full charge-based expression of drain current in all regions of operation of the MOSFET. In saturation, when $i_r \ll i_f$, (1) reverts to $I_D \simeq I_{spec} \cdot i_f$, which can be also stated as,

$$IC = \frac{I_D|_{sat.}}{I_{spec}} = \frac{I_D|_{sat.}}{I_0 \cdot \left(\frac{W}{L}\right)} \quad (8)$$

where IC is the inversion coefficient, with $IC < 0.1$, $0.1 < IC < 10$, and $IC > 10$ defining weak, moderate, and strong inversion, respectively.

In the following, the GCC method to extract threshold voltage at any level of inversion will be established. A first interesting observation is that when current components due to drift $i_{drift} = q_s^2$ and diffusion $i_{diff} = q_s$ are equal (i.e. $q_s^2 = q_s = 1$), then from (1) we have $IC = 2$, and from (3), $v_p - v_s = 2$, i.e. $v_p = v_s + 2$. Hence, biasing the transistor at $IC = 2$ allows us to obtain V_P simply as an offset from V_S , namely, $V_P = V_S + 2U_T$. We note at this point that for reasons of practicality, the slight dependence of specific current I_{spec} on slope factor n (and hence on V_G) is neglected: I_0 is assumed constant, and hence, a constant value of IC also implies a constant current I_D .

The procedure of determining threshold voltage and other substrate effect parameters is illustrated in Fig. 1. The current criterion of $IC = 2$ is applied to $I_D - V_G$ characteristics in saturation, with varying V_S . The intercepts with $IC = 2$ occur at specific gate voltages V_G , defining the pinchoff voltage characteristic as $V_P = V_S + 2U_T$. From the latter, the slope

TABLE I
CONSTANT CURRENT LEVELS AND PINCHOFF VOLTAGE OFFSET

$IC = q_s^2 + q_s$	$q_s = \sqrt{\frac{1}{4} + IC} - \frac{1}{2}$	$v_p - v_s = 2q_s + \ln(q_s)$
100	9.51	21.28
30	5	11.6
10	2.7	6.4
2	1	2
0.608	0.426	0
0.1	0.092	-2.2
10^{-2}	0.0099	-4.6
10^{-4}	$\approx 10^{-4}$	-9.21

factor n is obtained by derivation. The threshold voltage is determined as $V_{TO} = V_G|_{V_P=0V}$, while the other substrate effect parameters Ψ_0 and γ are obtained by a simultaneous fit of equations for V_P (4) and n (7) to the measured (or TCAD simulated) characteristics.

The procedure is equally applied to TCAD data as well as to the charge-based model, using the same parameters quoted in Fig. 1. The charge-based model (1)-(4) fits the TCAD data perfectly well, with the model using the same parameters as in the TCAD simulation. Technology parameters correspond to 180 nm CMOS technology.

When generalizing the above procedure to any value of IC , we can obtain the pinchoff voltage V_P from (1) and (3) as a function of IC and V_S ,

$$V_P = V_S + U_T \left(2 \left[\sqrt{\frac{1}{4} + IC} - \frac{1}{2} \right] + \ln \left[\sqrt{\frac{1}{4} + IC} - \frac{1}{2} \right] \right) \quad (9)$$

Some practical values of (9) are listed in Table I. In particular, we note that the condition $V_P = V_S$, corresponding to $IC = 0.608$, has been exploited in [4] and [5]. In [5], extraction of threshold voltage has also been extended to the case of non-saturation.

The generalized constant current method is illustrated in Fig. 2, showing the extraction procedure for a range of IC values from very weak ($IC = 10^{-4}$) to very strong ($IC = 100$) inversion. The V_P vs. V_G characteristics obtained for the different levels of IC are seen to practically overlap. The threshold voltage is again determined as $V_{TO} = V_G|_{V_P=0V}$, yielding the same value of V_{TO} for different levels of IC . The

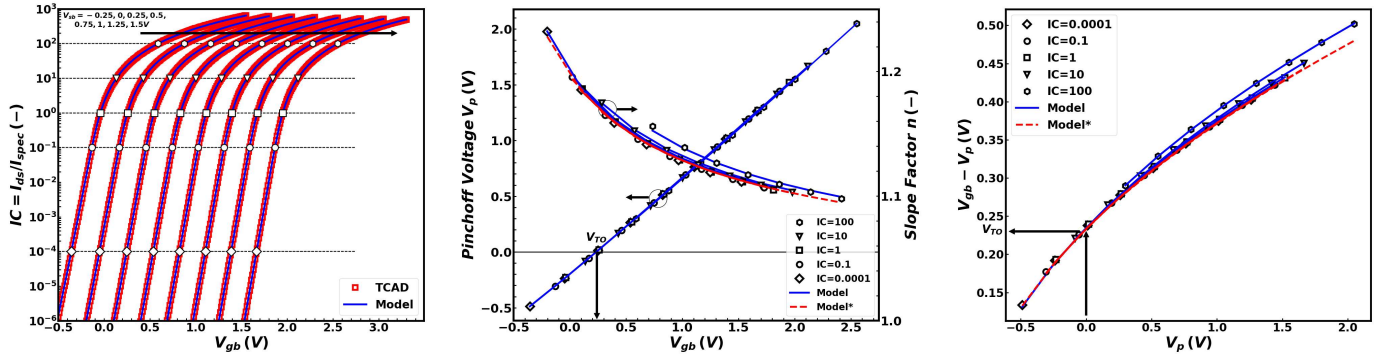


Fig. 2. Generalized constant current (GCC) method, obtained at values of $IC = I_D / (I_0(W/L))|_{I_0=cst.}$ ranging from very weak ($IC = 10^{-4}$) to very strong ($IC = 100$) inversion. Transfer characteristics with applied constant current (left), extracted pinchoff voltage V_P and slope factor n vs. V_G (center), and V_{TH} vs. V_P (right) of a wide/long n-MOSFET in saturation. V_{TO} is determined as $V_G|_{V_P=0}$ consistently for all values of IC . The GCC method is applied in the same way to TCAD data (markers) and charge-based model (lines). As I_0 is kept constant for the determination of the constant current criterion, a slight shift in n vs. V_G and V_{TH} vs. V_P characteristics is observed at $IC > 10$ consistently for TCAD data and model. This deviation is absent (red dashed line, Model*), when the charge-based model also uses constant I_0 .

slope factor n , which is a derivative quantity, is shown to be more sensitive, and presents a slight increase when IC values reach very high levels of inversion. This may be attributed to the fact that the dependency of the drain current I_D on the slope factor n (via I_{spec}) has been neglected in the extraction procedure. Indeed, when setting the slope factor to a constant value $n_0 = n|_{V_G=V_{TO}}$ in I_{spec} of the charge-based model, the GCC procedure yields the same slope factor at any level of IC , as indicated in Fig. 2 by dashed lines, coinciding for all levels of IC . Hence, the generalized constant current method and the charge-based model are self-consistent. In other words, the GCC method is applicable in strong inversion if the dependence of the biasing current on the slope factor n is anticipated. This is however not very practical, since when applying the CC criterion, the slope factor n should be known beforehand. In practice, IC values in moderate and weak inversion will be preferred, where the impact of mobility reduction due to vertical field or velocity saturation effects are reduced. In general, the choice of the level of the current criterion may depend on device particularities, such as leakage, or testing conditions or equipment that might restrict the current range.

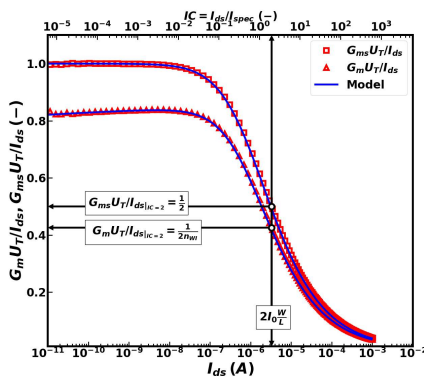


Fig. 3. Normalized transconductance-to-current ratio g_{ms}/i_d and g_m/i_d vs. drain current I_{ds} and IC (TCAD: markers, model: lines). The specific current $I_{spec} = I_0(W/L)$ is determined from a given fraction of g_{ms}/i_d or g_m/i_d . Here, $IC = 2$ is obtained corresponding to the drain current I_D where 50% of the maximum g_{ms}/i_d or g_m/i_d in weak inversion is attained.

To apply a (generalized) constant current criterion in the method as described above, one must first determine the specific current I_{spec} . This may be done from strong inversion conditions, e.g. described in [4]. Another possibility, particularly for low-current applications, exploits transconductance-to-current ratio characteristics at moderate levels of inversion. The normalized source and gate transconductance-to-current ratios, g_{ms}/i_d and g_m/i_d , are expressed [5],

$$\frac{g_{ms}}{i_d} = \frac{n g_m}{i_d} \Big|_{sat.} = \frac{1}{1 + q_s} = \frac{1}{\frac{1}{2} + \sqrt{\frac{1}{4} + IC}} \quad (10)$$

where $g_{m(s)} = +(-)\partial I_D / \partial V_{G(S)} \cdot U_T / I_{spec}$ are the normalized gate(source) transconductances. A certain level of $g_{m(s)}/i_d$, namely 61.8% of its maximum value in weak inversion, corresponds to $IC = 1$ [5]. Setting drift and diffusion currents to the same value corresponds to $IC = 2$. As is shown in Fig. 3, $IC = 2$ corresponds to 50% of the maximum of $g_{m(s)}/i_d$ via (10) (neglecting the slight bias dependence of the slope factor n). A resembling procedure in non-saturation ($i_f \approx i_r$) has been described [10].

III. APPLICATION OF GCC TO EDGE CONDUCTION

Shallow trench isolation (STI) is the preferred isolation scheme in advanced CMOS technology. As illustrated in Fig. 4, the STI regions at the side edges of the MOSFETs present a lower channel doping concentration due to dopant segregation, and possible thinning of the thin oxide [11]. As a result, the so-called edge transistors, which operate in parallel to the center transistor, may dominate the subthreshold conduction, strongly impacting on analog circuit operation [11] [13]. The edge and center transistors have a width of W_e and $W - W_e$, respectively, and the same channel length L , resulting in,

$$I_D = I_0 \cdot \left[\frac{W - W_e}{L} (i_f - i_r) + \frac{W_e}{L} (i_{fe} - i_{re}) \right] \quad (11)$$

where the same technology current I_0 has been assumed for both components. The current of the edge transistor is obtained using a separate set of equations of the charge-based model

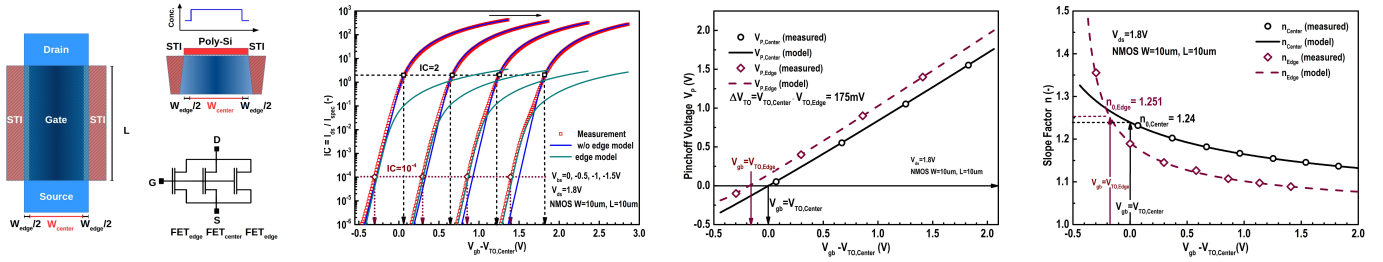


Fig. 4. Application of the GCC method in presence of edge conduction phenomenon in STI MOSFETs. Width of center and edge transistors sum up to the total width $W = W_c + W_e$, while all regions share the same length L . Transfer characteristics of a wide/long n-MOSFET in saturation at different back-bias at room temperature (measured data: markers) show edge conduction effect at inversion levels below $IC \approx 1$. Models (full and dashed lines) for the current of the center and edge transistors are shown. A constant current is applied to determine pinchoff voltage for the center transistor in moderate inversion at $IC = 2$. To characterize the edge transistor, imposing a current criterion $IC = 10^{-4}$ corresponds to $IC_e \approx 0.02$. Pinchoff voltage V_P and slope factor n characteristics illustrate the determination of parameters for center and edge transistors.

(1)-(4) and (7) with the edge transistor's parameters, $V_{TO,e}$, γ_e , Ψ_{0e} . This modeling approach has been used in the EKV3 compact MOSFET model [14], and was later adopted in the BSIM-Bulk model [15].

The specific current and inversion coefficient of the edge transistor are related to that of the central transistor as,

$$\frac{I_{spec,e}}{I_{spec}} = \frac{W_e}{W - W_e}, \quad \frac{IC_e}{IC} = \frac{W - W_e}{W_e}. \quad (12)$$

When applying the GCC method to a transistor with edge conduction effect, a suitable current criterion must be chosen above the level where the hump is apparent, to determine parameters of the central transistor. This could be significantly higher than $IC = 2$ used here, particularly in narrow transistors. Conversely, a level well below $IC = 0.1$ may be needed for the characterization of the edge transistor. For the latter, it is naturally important that the inversion coefficient IC_e (12) is used instead of IC in (9). Fig. 4 illustrates the significant shift in threshold voltage and reduction in slope factor n for the edge transistor w.r.t. the central transistor. Here, the current criterion of $IC = 10^{-4}$ of the central transistor corresponds to $IC_e \approx 0.02$ of the edge transistor.

IV. CONCLUSION

A new generalized constant current (GCC) method allows for the extraction of MOSFET threshold voltage and other substrate effect-related parameters, from measured drain current at any inversion level from weak to strong inversion. The GCC method is intricately related to the charge-based model of the MOSFET but may be applied to many other models. A constant current criterion $I_{D,gcc} = I_0 \cdot (W/L) \cdot IC$, where IC defines the desired level of inversion, is typically applied to saturated $I_D - V_G$ characteristics of MOSFETs. Weak ($IC < 0.1$) and moderate ($0.1 < IC < 10$) levels of inversion are preferable due to reduced high-field effects. Pinchoff voltage vs. V_G , or threshold voltage vs. V_S characteristics are obtained, from which V_{TO} and other substrate effect parameters may be determined, irrespectively of the chosen level of inversion IC . As an example, the GCC method is applied to the edge conduction effect in STI-isolated MOSFETs.

REFERENCES

- [1] H.-G. Lee, S.-Y. Oh, and G. Fuller, "A simple and accurate method to measure the threshold voltage of an enhancement-mode MOSFET", *IEEE Trans. Electron Devices*, vol. 29, no. 2, pp. 346-348, Feb. 1982. doi: [10.1109/T-ED.1982.20707](https://doi.org/10.1109/T-ED.1982.20707).
- [2] M. J. Deen and Z. X. Yan, A new method for measuring the threshold voltage of small-geometry MOSFETs from subthreshold conduction, *Solid State Electron.*, vol. 33, no. 5, pp. 503511, 1990. doi: [10.1016/0038-1101\(90\)90234-6](https://doi.org/10.1016/0038-1101(90)90234-6).
- [3] A. Ortiz-Conde, F. J. Garcia-Sanchez, *et al.*, Revisiting MOSFET threshold voltage extraction methods, *Microelectron. Reliab.*, vol. 53, no. 1, pp. 90104, 2013. doi: [10.1016/j.microrel.2012.09.015](https://doi.org/10.1016/j.microrel.2012.09.015).
- [4] M. Bucher, C. Lallement and C. Enz, "An efficient parameter extraction methodology for the EKV MOST model", in *IEEE Int. Conf. Microelectronic Test Structures (ICMETS)*, 1996. doi: [10.1109/ICMETS.1996.535636](https://doi.org/10.1109/ICMETS.1996.535636).
- [5] A. Bazigos, M. Bucher, J. Assenmacher, *et al.*, An adjusted constant-current method to determine saturated and linear mode threshold voltage of MOSFETs, *IEEE Trans. Electron Devices*, vol. 58, no. 11, pp. 37513758, Nov. 2011. doi: [10.1109/TED.2011.2164080](https://doi.org/10.1109/TED.2011.2164080).
- [6] J.-M. Sallese, M. Bucher, F. Krummenacher, and P. Fazan, Inversion charge linearization in MOSFET modeling and rigorous derivation of the EKV compact model, *Solid-State Electron.*, vol. 47, no. 4, pp. 677683, 2003. doi: [10.1016/S0038-1101\(02\)00336-2](https://doi.org/10.1016/S0038-1101(02)00336-2).
- [7] C. Enz and E. Vittoz, Charge-based MOS transistor modeling, John Wiley and Sons, Chichester, 2006. doi: [10.1002/0470855460](https://doi.org/10.1002/0470855460).
- [8] C. Enz, F. Krummenacher, and E. Vittoz, "An analytical MOS transistor model valid in all regions of operation and dedicated to low-voltage and low-current applications", *Analog Integr. Circuits Signal Process.*, vol. 8, pp. 83-114, 1995. doi: [10.1007/BF01239381](https://doi.org/10.1007/BF01239381).
- [9] C. Lallement, M. Bucher, and C. Enz, "Modelling and characterization of non-uniform substrate doping", *Solid-State Electron.*, vol. 41, no. 12, pp. 1857-1861, 1997. doi: [10.1016/S0038-1101\(97\)00137-8](https://doi.org/10.1016/S0038-1101(97)00137-8).
- [10] O. F. Siebel, M. C. Schneider, and C. Galup-Montoro, "MOSFET threshold voltage: definition, extraction, and some applications", *Microelectron. J.*, vol. 43, no. 5, pp. 329336, May 2012. doi: [10.1016/j.mejo.2012.01.004](https://doi.org/10.1016/j.mejo.2012.01.004).
- [11] P. Sallagoity, M. Ada-Hanifi, M. Paoli, and M. Haond, "Analysis of width edge effects in advanced isolation schemes for deep submicron CMOS technologies", *IEEE Trans. Electron Devices*, vol. 43, no. 11, pp. 1900-1996, Nov. 1996. doi: [10.1109/16.543025](https://doi.org/10.1109/16.543025).
- [12] Y. Joly, L. Lopez, *et al.*, "Impact of hump effect on MOSFET mismatch in the sub-threshold area for low power analog applications," in *IEEE Int. Conf. Solid-State and Integrated Circuit Technology (ICSITC)*, 2010. doi: [10.1109/ICSITC.2010.5667684](https://doi.org/10.1109/ICSITC.2010.5667684).
- [13] K. Sakakibara, T. Kumamoto, and K. Arimoto, "Impact of subthreshold hump on bulk-bias dependence of offset voltage variability in weak and moderate inversion regions", in *IEEE Custom Integrated Circuits Conf. (CICC)*, 2012. doi: [10.1109/CICC.2012.6330574](https://doi.org/10.1109/CICC.2012.6330574).
- [14] A. Bazigos, M. Bucher, F. Krummenacher, J.-M. Sallese, *et al.*, "EKV3 compact MOSFET model documentation, model version 301.02, Technical Report, Technical University of Crete, Chania, Greece, July 2008.
- [15] S. Khandelwal, H. Agarwal, *et al.*, "Modeling STI edge parasitic current for accurate circuit simulations," *IEEE Trans. Comput.-Aided Design Integr. Circuits Syst.*, vol. 34, no. 8, pp. 1291-1294, Aug. 2015. doi: [10.1109/TCAD.2015.2419626](https://doi.org/10.1109/TCAD.2015.2419626).